Desalination and Water Treatment
www.deswater.com

doi: 10.1080/19443994.2013.769743

51 (2013) 5863–5872
August

Taylor & Francis
Taylor & Francis Group

Batch and column studies on the evaluation of micrometer and nanometer Phragmites australis for nitrate removal

Masoumeh Farasati[a]*, Morteza Seyedian[b], Saeed Boroomandnasab[c]
Nemat. Jaafarzadeh[d], Hadi Moazed[c], Houshang Ghamarnia[a]

[a]*Faculty of Agriculture, Department of Irrigation and Water Resources Engineering, Razi University, P.O. Box. 1158, Kermanshah, Post code: 6715685438, Iran Fax: 0988318323727; email: farasati2760@gmail.com*
[b]*Department of Watershed Management, College of Agriculture, Gonbad Kavoos University, Gonbad Kavoos, Iran*
[c]*Faculty of Water Sciences Engineering, Shahid Chamran University, Ahvaz, Iran*
[d]*Environmental Technology Research Center, Ahvaz Jundi Shahpur University of Medical Sciences, Ahvaz, Iran*

Received 25 March 2012; Accepted 20 December 2012

ABSTRACT

The effects of Phragmites australis anion exchanger (PHA-AE) with micrometer and nanometer scales as adsorbents for nitrate removal were investigated. Also, the effects of operating conditions including pH, contact time, adsorbent loading, initial anion concentrations, and desorption experiments were examined. The results showed that the optimum pH was equal to 6 as the equilibrium time were 3 and 2 h for micrometer and nanometer PHA-AE, respectively. With the increased nitrate concentrations (5, 15, 50, 80, and 120 mg/L) for micrometer and nanometer PHA-AE, q_e (adsorption capacity) increased from 0.4 to 6.97 mg/g and 0.45 to 7.7 mg/g. With increase of adsorbents dose from 0.1 to 0.3 g, the percentage of nitrate removal increased from 47 to 56% and 54 to 68% for microstructure and nanostructure adsorbent, respectively; however, the percentage of removal remained almost constant with the adsorbent dosage ranging from 0.3 to 1 g. The adsorption of nitrate ions onto PHA-AE was described successfully by pseudo-second-order adsorption kinetic and Langmuir–Freundlich adsorption isotherm. The results of the present study indicated that PHA-AE may be used to remove nitrate ions from water treatment process. PHA-AE nanometer showed greater capability of nitrate adsorption, too, as compared to PHA-AE micrometer adsorbent.

Keywords: Phragmites australis; Nitrate removal; Nanometer adsorbent; Micrometer adsorbent

1. Introduction

Nitrate pollution in surface water and groundwater resources is becoming a troublesome issue to address across the world. High concentrations of nitrate usually lead to the formation of nitrosamine, which causes cancer and increases the risks of diseases to spread including blue baby in infants [1]. The removal of contaminants and recycling of the purified water provide substantial reductions in cost, time, and labor to the industry and result in an improved environmental stewardship [2]. Sorbents are widely used as separation media in water purification processes to remove organic and inorganic pollutants from contaminated water resources [3,4].

In wastewater treatment industries, various techniques, including chemical and biological methods

---

*Corresponding author.

such as reverse osmosis [5]; biological de-nitrification [6]; electrodialysis [3], and anion exchange [7], have been successfully applied. Among these methods, anion exchange is proven to be a feasible process for *in situ* treatment of underground and surface water primarily due to its ease of application [3]. Recently, numerous efforts have been made to find effective and economical anion exchangers obtained from agricultural by-products. Therefore, several materials such as sugarcane bagasse [8] and peanut hull [9] may be modified to anion exchangers and used for this purpose. However, there has been no report on the use of processed Phragmites australis (PHA) as anionic sorbent in literature. Research is underway to use advance nanotechnology in water purification for safe drinking. Nanoparticles are expected to play a crucial role in water purification [10]. They have much larger surface area than bulk particles. It has also been found that the unique properties of nanoparticles normally develop high capacities and selective sorbents for metal ions and anions [11]. In the present study, the main goal is prepare an anionic sorbent from PHA with scale micrometer and nanometer, and their characterization for the adsorption of nitrate from aqueous solution.

2. Materials and methods

2.1. Preparation of Phragmites Australis-Anion Exchanger

The synthesis process for Phragmites Australis-Anion Exchanger (PHA-AE) was divided into two steps; aminated intermediate was synthesized as the first step. An aliquot of 78 mL (1 mol) of epichlorohydrin was reacted with 152 mL (1.1 mol) of triethylamine in 150 mL of 50/50 (v/v)% methanol solution at 55℃. After being stirred for 5 h, the produced intermediate was used, as the second step. During the second synthesis process, 5 g of PHA were reacted with 35 mL of intermediate and 5 ml of pyridine in a 250 mL three-neck round bottom flask for 3 h at 55℃ [12]. The product was washed with distilled water to remove the residual chemicals, dried at 60℃ for 12 h and sieved to obtain particles with microstructure and nanostructure scales.

2.1.1. Characteristics of adsorbent

Surface morphology of the PHA and PHA-AE adsorbent was investigated by scanning electron microscope. The size of microparticles was examined by sieving while the size of nanoparticles was determined by the use of particle size analyzer (PSA). Total nitrogen content of the final product was determined by Perker-Elmer Elemental analyzer CHNS/O. The total exchange capacity (TEC) was calculated based on the nitrogen content that was incorporated into the final products as specified in equation below [13]:

$$\text{TEC (meq g}^{-1}\text{)} = \frac{\text{N\%}}{1.4} \tag{1}$$

where TEC is total exchange capacity and N is nitrogen content in percent.

2.2. Chemicals

Fifteen mg/L of nitrate stock solution were prepared by dissolving the required weighed quantities (24.46 mg) of KNO_3 in distilled water. All solutions for the sorption and subsequent analysis were prepared by an appropriate dilution of the freshly prepared stock solution.

PHA-AE by-product is a potential alternative as an anion exchanger because of its particular properties including chemical stability and high reactivity resulting from the presence of reactive aminated groups in polymer chains. For each 30 mL centrifuge tube, 0.3 g of PHA-AE and 30 mL of working solution were mixed together for 3 h at 120 rpm. Then the mixtures were centrifuged and filtered by using filter paper to separate water from the absorbent. NO_3^- was analyzed by a UV-Vis spectrophotometer (Hach model, DR5000). All the samples were prepared in triplicate and NO_3^- exchanged on PHA-AE was determined by equation below:

$$q_e = \frac{C_i - C_f}{m} \times V \tag{2}$$

where q_e is NO_3^- exchanged on PHA-AE (mg/g), m is the adsorbent mass (g), C_0 and C_e is the initial and equilibrium concentrations of NO_3^- in solution (mg/L) and V is solution volume (L), respectively. The removal efficiency was evaluated by the following equation:

$$R = \frac{C_i - C_f}{C_i} \times 100 \tag{3}$$

where R is nitrate removal efficiency expressed in percent.

2.2.1. pH studies

In order to investigate the effects of pH on nitrate adsorption, pH values of KNO_3 solutions (i.e. 15 mg/L NO_3^-) were adjusted in the range from 2 to 10. The initial pH value of solution was adjusted by using H_2SO_4 or NaOH (0.1 N). Then, 0.3 g dried PHA-AE was added to the solution. After adsorption, pH value with maximum nitrate removal was determined.

Zero point charge (pH_{pzc}) of the adsorbent is an important parameter in the adsorption of anions. The value of pH_{pzc} is defined by the point at which the curve pH_{final} vs. $pH_{initial}$ crosses the line $pH_{final} = pH_{initial}$. The procedure was repeated for all other samples. Blank tests without adsorbent were also conducted in order to eliminate the impact of CO_2 from air on pH [14].

2.2.2. Effect of contact time

In kinetic studies, 30 mL KNO_3 solution and 0.3 g adsorbent were agitated. The mixtures were shaken at 120 rpm and the batch experiments were repeated for different periods from 10 to 210 min until the adsorption equilibrium was reached.

2.2.3. Effect of adsorbent dosage

The adsorption of 15 mg/L of NO_3^- solution by different adsorbent doses (0.1–1.0 g) for each adsorbent was carried out at the optimum value of pH and contact time.

2.2.4. Effect of initial concentration

The effects of initial concentrations on the adsorption of NO_3^- ions by PHA-AE were evaluated with varying nitrate concentrations (5, 15, 50, 80, and 120 mg/L) at the optimum value of pH, time, and adsorbent dosages.

2.3. Equilibrium adsorption isotherm

The equilibrium adsorption data were analyzed by using different isotherm models to understand the adsorbate–adsorbent interactions. In order to characterize the exchange equilibrium of NO_3^- ions by PHA-AE, the Freundlich, Langmuir, Redlich–Peterson, and Langmuir–Freundlich models were used as follows [15]:

Freundlich equation:

$$q_e = KC_e^{1/n} \tag{4}$$

Langmuir equation:

$$q_e = \frac{bq_m C_e}{(1 + bC_e)} \tag{5}$$

Redlich–Peterson equation:

$$q_e = \frac{aC_e}{(1 + bC_e^n)} \tag{6}$$

Langmuir–Freundlich equation:

$$q_e = \frac{bq_m C_e^{1/n}}{(1 + bC_e^{1/n})} \tag{7}$$

where q_e is the amount of nitrate exchanged at equilibrium ($mgNO_3^-/g$) and C_e is the nitrate equilibrium concentration in solution (mg NO_3^-/L). The other parameters represent different isotherm constants that may be determined by regression of the experimental isotherm data. According to the literature, the nonlinear regression analysis method is a more efficient method in obtaining parameters involved in three parameter isotherms than other known methods [16]. Hence, the ion exchange isotherms were examined by the nonlinear curve fitting analysis method using Data-fit software [17].

The dimensionless parameter or separation factor, R_L, based on the more analysis of the Langmuir equation, may be determined in the following equation [18]:

$$R_L = \frac{1}{1 + bC_0} \tag{8}$$

where C_0 (mg/L) is the initial concentration of exchangeable ion and b is the Langmuir constant. The parameter of R_L is considered as a more valid indicator of ion exchange. The value of R_L may be determined for four cases: [27]: (1) favorable exchange, $0 < R_L < 1$, (2) unfavorable exchange, $R_L > 1$, (3) linear exchange, $R_L = 1$, and (4) finally, irreversible exchange, $R_L = 0$.

In the present work, the best fit between experimental and model estimated data was evaluated by R^2 and the RMSE as follows:

$$\mathrm{RMSE} = \sqrt{\frac{\sum_{i=1}^{n} (q_e - q_c)^2}{n}} \tag{9}$$

where q_e and q_c are the measured and model estimated amounts of NO_3^- exchanged, respectively, and n is the number of measurements. A lower RMSE value and higher R^2 value show the best fit of agreement between the measured and estimated NO_3^- exchanged data.

2.4. Kinetic study

The adsorption rate of nitrate was studied at different time intervals for 210 min by using 120 mg/L initial concentrations at optimum value of pH. The modeling of the kinetics of NO_3^- adsorption on PHA-AE was checked by three common models, Eqs. (10)–(13), as described below [19]:

Pseudo-first-order equation:

$$q_t = q_e(1 - e^{-k_1 t}) \tag{10}$$

Pseudo-second-order equation:

$$q_t = \frac{q_e^2 k_2 t}{1 + q_e k_2 t} \tag{11}$$

Power equation:

$$q_t = at^b \tag{12}$$

Elovich equation:

$$q_t = \left(\frac{1}{\beta}\right)\ln(\alpha\beta) + \left(\frac{1}{\beta}\right)\ln t \tag{13}$$

where q_t is the amount of nitrate removed during time t (mg NO_3^-/g), q_e is the amount of nitrate removed at equilibrium state, and k_1, k_2, α, β, a, and b are constants. R^2 and RMSE were determined for different models, and lower RMSE value and higher R^2 value were considered to represent goodness of conformity between the measured and estimated NO_3^- removed data.

2.5. Desorption studies

After adsorption experiments were carried out and the solution separates from the absorbent the desorption of the adsorbed nitrate was studied by shaking the spent modified PHA-AE with 30 mL of 0.1 mol/L HCl for an optimum contact time. After a specific period of time, the sorbent was filtered and desorbed nitrate concentration was analyzed by UV-Vis spectrophotometer. The percentage of desorbed (D) nitrate anion was obtained by the following:

$$\text{Desorption } (\%) = \frac{\text{desorbed amount of solute}}{\text{absorbed amount of solute}} \times 100 \tag{14}$$

2.6. Column experiment

The sorption in a continuous-flow system was carried out in a fixed bed column reactor (2.8 cm i.d., 35 cm column length). Filters of 40 μm diameter were used at the top and the bottom of sorbent. Feed water was made with KNO_3^- solution, having an initial concentration of 15, 50 with 120 mg/L nitrate. Once the column was saturated with water, no visual evidence of air pockets remaining inside the column was observed. The water was pumped upwards into the column by using a peristaltic pump at 0.98 and 2.27 L/hr flow rates. Samples were collected from the exit of the column at 30-min intervals and were further analyzed for nitrate.

3. Results and discussion

The characteristics of PHA-AE showed that a number of aminated groups were grafted in the structure of PHA-AE which results in nitrate removal (Fig. 1).

Table 1 displays the elemental changes of carbon, hydrogen, and nitrogen in PHA-AE as compared to PHA. The significant increase in nitrogen content (0.75–3.96%) of PHA-AE indicates the reactions between phragmites australis and aminated intermediate. Also, a number of aminated groups have been produced into PHA-AE. Identical results were presented in a work by Xing for the preparation of anion exchangers from wheat straw as having nitrogen content in a range of 0.35–3.57% and Gao for the preparation of anion exchangers from coin, rice hull, pure alkaline lignin, and sugarcane bagasse as having nitrogen contents in a range of 3.6–5.8% [20,12].

The results of PSA analysis on PHA-AE nanometer are shown in Fig. 2. They indicate that 81.5% of particles had a size below 406 nm while 18.5% of them were below 51.47 nm. The particle size distribution of PHA-AE shows a satisfactory bell-shaped distribution curve (Fig. 2). The size of micrometer adsorbent obtained by sieving 50 mesh number was 330 μm.

3.1. Adsorption studies

3.1.1. Effect of initial pH

Fig. 3 shows variations in the amounts adsorbed as a function of initial pH values for nitrate anion. With pH values of the solution varying from 2 to 10, $R\%$ and q_e values of micrometer PHA-AE increased up to the maximum of 43–73% and 0.85–1.46 mg/g, respectively. For nanometer-sized PHA-AE, $R\%$ and q_e values increased up to the maximum of 53–85% and 1.05–1.69 mg/g. The increase of nitrate adsorption by PHA-AE as a result of increased electrostatic interactions between PHA negatively charged nitrate groups and positively charged aminated groups. Thus, the optimum pH value of nitrate removal was obtained as 6.0. The adsorption dependence on pH value shows ion exchange mechanism of nitrate removal [21].

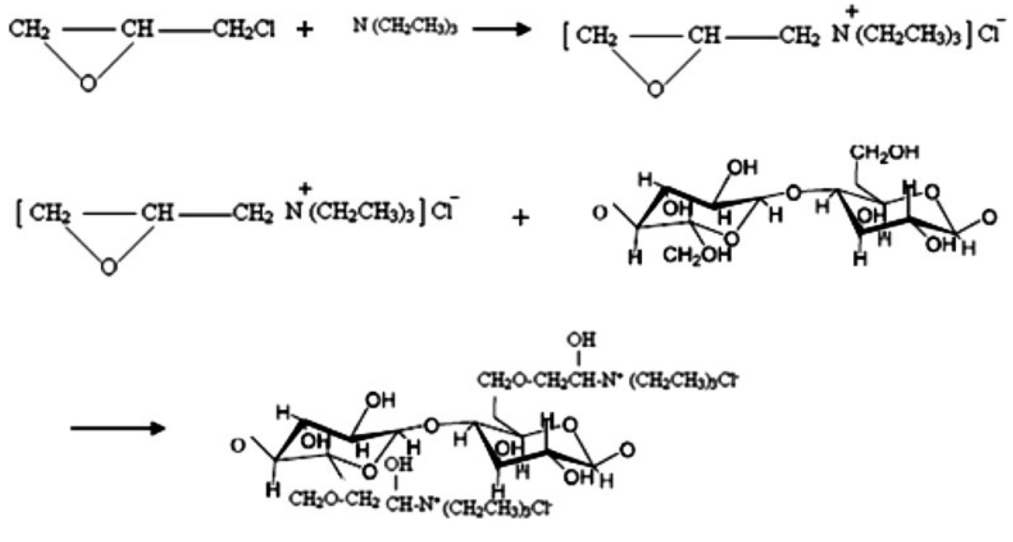

Fig. 1. Synthetic reactions of PHA-AE.

Table 1
Elemental change in raw and modified PHA adsorbent

Adsorbent	C%	H%	N%	TEC
PHA	37.2	5.31	0.75	0.54
PHA-AE	38.2	5.77	3.96	2.83

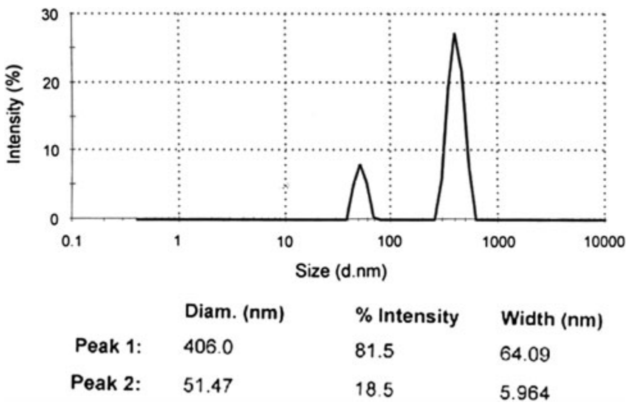

	Diam. (nm)	% Intensity	Width (nm)
Peak 1:	406.0	81.5	64.09
Peak 2:	51.47	18.5	5.964

Fig. 2. The particle size distribution of PHA-AE-nanostructure.

3.1.2. Effect of contact time

Fig. 4 shows variations in the adsorbed amounts as a function of time for nitrate anion with time changing from 10 to 210 min. The values of $R\%$ and q_e of micrometer-sized PHA-AE increased up to maximum of 31–78% and 0.465–1.095 mg/g reached at 3 h, respectively while for nanometer-sized PHA-AE, $R\%$ and q_e increased up to maximum of 46–86% and 0.69–1.29 mg/g reached at 2 h, respectively.

3.1.3. Effect of adsorbent dosage

For PHA-AE micrometer and nanometer, and the increase of the adsorbent dosages from 0.1 to 0.3 g, $R\%$ increased from 41 to 71% and 56–83% reaching a maximum of 71 and 83% in 0.3 g adsorbent, respectively; however, it remained almost unchanged with adsorbent dosage ranging from 0.3 to 1 g (Fig. 5). In general, the increase of adsorbent dosage led to an increased percentage of nitrate removal, which was caused by an increase of adsorbent surface area and more adsorption sites of the adsorbent. At adsorbent dosage of >0.3 g, the extra NO_3^- ion removal becomes very low, hence, the increased adsorbent dosage did not enhance the removal percentage of NO_3^- ion.

3.1.4. Effect of initial concentration

The effects of initial concentrations on the adsorption of NO_3^- ions by PHA-AE were investigated with varying nitrate concentrations of 5, 15, 50, 80, and 120 mg/L using 0.3 g adsorbent dose (Fig. 6). With the increase of solution concentration for PHA-AE micrometer and nanometer, the value of q_e increased from 0.4 to 6.97 mg/g and 0.45 to 7.7 mg/g while $R\%$ from 80 to 61% and 90–67% decreased. At low initial nitrate concentrations, the surface area and the availability of adsorption sites were relatively high, and the NO_3^- ions were easily adsorbed and removed. The initial high rate of nitrate uptakes were probably due to greater availability of binding sites near the surface of the PHA-AE adsorbent. At higher initial amounts of nitrate concentrations, the total available adsorption sites were limited, hence, it resulted in a decreased removal percentage of NO_3^- ions. The increased q_e at

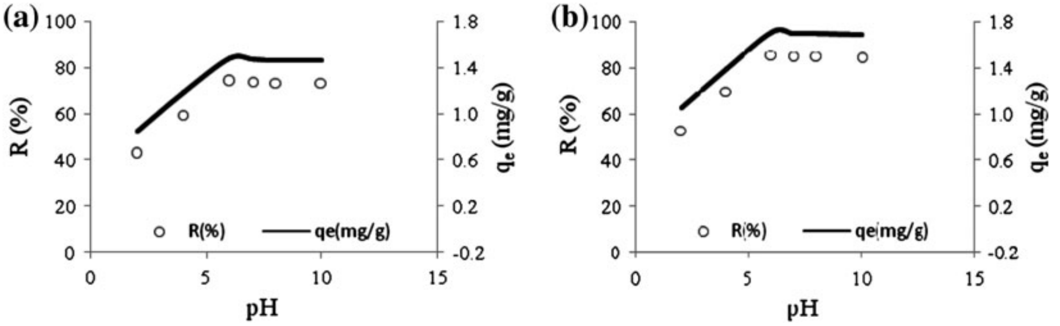

Fig. 3. Effect of pH on the adsorption of NO_3^- ion by PHA-AE (a) micrometer-sized (b) nanometer-sized adsorbent (anion initial concentration: 15 mg/L, adsorbent loading: 0.3 g, adsorption time: 3 h).

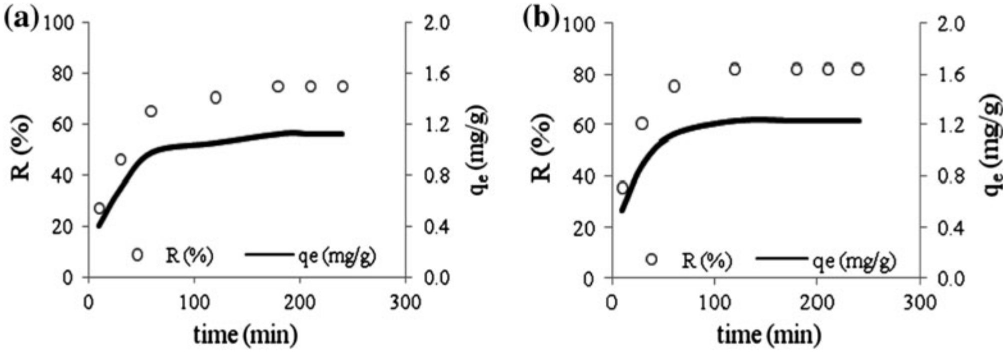

Fig. 4. Effect of contact time on the adsorption of NO_3^- ion by PHA-AE adsorbent (a) micrometer-sized (b) nanometer-sized (anion initial concentration: 15 mg/L, adsorbent loading: 0.3 g, pH = 6).

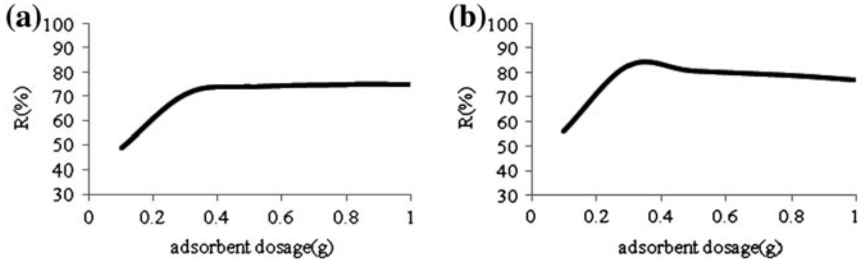

Fig. 5. Effect of adsorbent dosage on removal of nitrate by PHA-AE adsorbent (a) micrometer (b) nanometer (anion initial concentration: 15 mg/L, pH = 6, t = 3 h, 2 h).

higher initial concentrations can be attributed to the enhanced driving force.

3.2. Nitrate exchange isotherms

Ion-exchange isotherms characterize the equilibrium relationship between the amounts of exchanged ions by PHA-AE and its equilibrium concentration in the solution [22]. In the present study, the ion exchange isotherms data obtained for micrometer- and nanometer-sized PHA-AE were fitted to the Freundlich, Langmuir, Redlich–Peterson, and Langmuir–Freundlich models. The estimated model parameters including R^2 and RMSE for the different models are presented in Table 2, indicating that the experimental data of NO_3^- exchange may be well fitted by all four models. Also, it became clear that the three-parameter models (Langmuir–Freundlich) provided better fitting with respect to R^2 and RMSE for all treatments as compared to the two-parameter isotherms (Freundlich and Langmuir). This result is supported by the findings of Malekian et al. (2011) [15]. However, the two-parameter equations are more extensively used in practice than the three parameter equations since they are difficult to

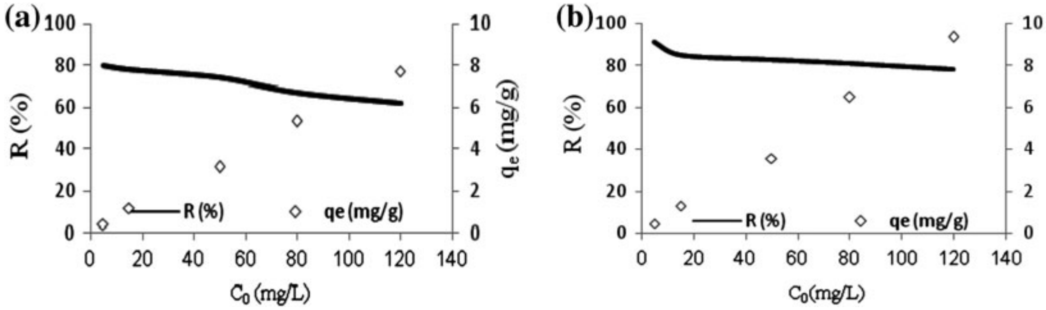

Fig. 6. Effect of initial concentration on the removal and adsorption of NO_3^- ions by PHA-AE (a) micrometer (b) nanometer (pH = 6, t = 3 h, 2 h, m = 0.3 g).

analyze the three parameters isotherm. For the two-parameter isotherms, Langmuir model provided more conforming results to the experimental data in comparison to Freundlich model. One of the important parameters in Langmuir equation is R_L. Fig. 7 shows the variations of R_L with initial concentrations of the NO_3^- ion for all the treatments. As seen from this figure, R_L parameters were found to be between 0 and 1 indicating the suitability of NO_3^- ions removal by PHA-AE. The R_L value obtained also demonstrates that PHA-AE was a potential ion exchanger for NO_3^- ion removal from aqueous solution. This is supported by the results of several studies in the literature [15,18]. Fig. 7 shows that R_L value approaches zero as C_0 value increases indicating that the exchange of NO_3^- ion onto PHA-AE is less favorable at high concentrations of NO_3^-. Therefore, Langmuir–Freundlich equation can describe nitrate removal by ion [18] exchange better than Langmuir or Freundlich equation. The other parameter q_m, used in either Langmuir or Langmuir–Freundlich equations represents NO_3^- ion exchange capacity [23] and is presented in Table 2 for micrometer- and nanometer-sized PHA-AE. It is generally accepted that q_m obtained from Langmuir–Freundlich equation can be more reasonable than that from Langmuir equation [23]. The comparison of q_m values for micrometer- and nanometer-sized PHA-AE suggests that the maximum NO_3^- exchange increases with the reduction of particle size (see Table 2). This is consistent with the results of Malekian et al., 2011 [15]. The maximum NO_3^- exchange capacity by the PHA at equilibrium was 30 and 32 mg NO_3^-/g for micrometer- and nanometer-sized PHA-AE, respectively (see Table 2). The constant of 1/n for the Freundlich isotherm ranges from 0 to 1 and is a measure of exchange intensity or surface heterogeneity with a value of 1/n smaller than 1 that indicates favorable removal conditions [24]. In this study, the value of 1/n (Freundlich constant) for PHA-AE ranged from 0.81 to 0.88 (Table 2) suggesting that the exchange conditions were actually favorable.

Table 2
Isotherm constants and statistical comparison values for NO_3^- exchange from solutions on micrometer- and nanometer-sized PHA-AE

Model	Micrometer-sized	Nanometer-sized
Fruendlich		
k	0.54	0.82
$1/n$	0.7	0.75
R^2	0.985	0.988
RMSE	0.296	0.253
Langmuir		
q_m(mg/g)	15.71	23.05
b(L/mg)	0.021	0.026
R^2	0.994	0.999
RMSE	0.236	0.222
Redlich–Peterson		
a	0.805	0.768
b	0.07	0.156
n	0.43	0.616
R^2	0.996	0.999
RMSE	0.233	0.205
Langmuir–Freundlich		
q_m(mg/ g)	30	35.573
b(Lm/g)	0.016	0.02
1/n	0.82	0.885
R^2	0.997	0.999
RMSE	0.177	0.144

3.3. Kinetic study

The estimated values of different parameters are presented in Table 3. As to micrometer- and nanometer-sized Phragmites australis, the R^2 values for pseudo-second-order model gives the best fit of 0.993 and 0.996 and RMSE values of 0.285 and 0.134, respectively: however, It is predicted that q_e values of 8.4 and 9.9 mg/g are overestimated as compared to the

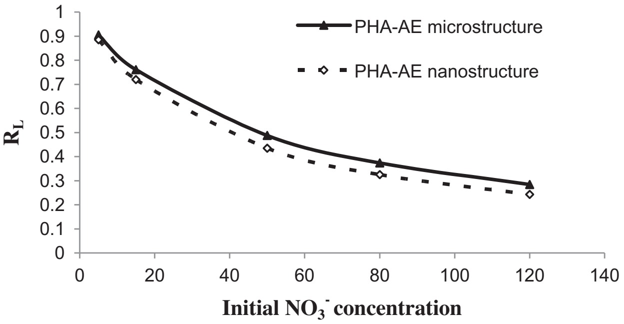

Fig. 7. Variation of separation factor (RL) as a function of initial NO_3^- concentration for PHA-AE of micrometer-sized and nanometer-sized.

experimentally observed values of 7.68 and 9.35 mg/g. In pseudo-first-order model, the predicted values of q_e of 5.87, 6.5 mg/g was lower than the experimentally observed values of 7.68, 9.35 mg/g. Nonetheless, q_e values estimated from the pseudo-second-order model are extrapolated outside the time period as experimentally investigated. The fact still remains that the pseudo-first-order model accurately predicts the adsorption kinetics throughout the experiments. The highest RMSE values obtained for the pseudo-first-order model were 1.89 and 2.904. Therefore, this model may be used to predict the kinetics of adsorption of NO_3^- on PHA-AE.

The power function model satisfactorily describes NO_3^- removed by micrometer- and nanometer-sized PHA-AE with RMSE: 0.75, 0.64, R^2: 0.84, 0.89, respectively (see Table 3).

The Elovich model determines the amount of NO_3^- removed by micrometer-sized and nanometer-sized PHA-AE with RMSE of 0.551, 0.366 and R^2: 0.901, 0.957, respectively (see Table 3). The results showed that the pseudo-first-order rate expression was not valid to be used in the studied systems (see Table 3). The calculated and experimental equilibrium uptake values fit well to pseudo-second-order rate model indicating that the pseudo-second-order reaction works more efficiently than pseudo-first-order reaction. By comparing micrometer- and nanometer-sized PHA-AE, one can infer that the nanometer particle-sized PHA-AE was fine, spherical, with high surface area while having high activity and adsorbing ions quickly. The results are in agreement with those obtained by Rahmani et al. [25]. It was also found that the fitting to pseudo-second-order model gave the highest determination coefficients (R^2), lowest RMSE and predicted q_e more accurately than the other models under study Therefore; pseudo-second-order model may be used to predict the kinetics of nitrate adsorption.

Table 3
Kinetic models parameters for the adsorption of NO_3^- on PHA-AE and 120 mg/L initial NO_3^- concentration (Co: mg/L; q_e: mg/g; k_1: min^{-1}; k_2: g/mg min, α: mg/g min and β: g/mg)

Model	Micrometer-sized	Nanometer-sized
Pseudo-first-order equation		
q_{exp}	7.68	9.35
k_1	0.023	0.032
q_e	5.87	6.5
R^2	0.984	0.989
RMSE	2.904	1.89
Pseudo-second-order equation		
K_2	0.006	0.01
q_e	8.4	9.9
R^2	0.996	0.993
RMSE	0.285	0.134
Power function		
a	1.51	2.92
b	0.317	0.228
R^2	0.84	0.89
RMSE	0.75	0.64
Elovich equation		
$\frac{1}{\beta}\ln(\alpha\beta)$	-0.55	1.48
$\frac{1}{\beta}$	1.59	1.54
R^2	0.901	0.957
RMSE	0.551	0.366

3.4. Desorption

The results of NO_3^- desorption by HCl are shown in Table 4 and one can observe that HCl demonstrates high desorption capacities; this indicates that Cl^- from the HCl solution displacing NO_3^- ion onto PHA-AE adsorbent.

4. Result of column experiment

4.1. Result of the change of equilibrium nitrate concentration with time

Figs. 8 and 9 show the variations in the equilibrium nitrate concentration as a function of time on micrometer- and nanometer-sized PHA-AE.

The results indicate that for micrometer-sized PHA-AE with flow rate of 0.98 and 2.27 L/h, exhaustion time was 270, 180, 120 min with 120, 90, 60 for 15, 50, and 120 mg/L of initial nitrate concentrations, respectively. For micrometer-sized PHA-AE with flow

Table 4
Desorption parameters of desorption solvent

Adsorbent	Adsorbed nitrate (mg/L)	Desorbed nitrate (mg/L)	Desorption efficiency (%)
Micrometer PHA-AE	11.7	8.25	70.51
Nanometer PHA-AE	12.88	10.02	77.8

rate of 0.98 and 2.27 L/h, the adsorption capacities (q_e) of 6.67, 14.63, 26.03 mg/g and 5.48, 12.26, 20.01 mg/g for 15, 50 and 120 mg/L of initial nitrate concentrations were obtained, respectively. For nanometer-sized PHA-AE with flow rate of 0.98 and 2.27 L/h, the exhaustion times was 360, 300, 240 min and 180, 120, 90 min for 15, 50 and 120 mg/L initial nitrate concentrations, respectively. For nanometer-sized PHA-AE with flow rate of 0.98 and 2.27 L/h, adsorption capacity (q_e) of 9.6, 30.2, 54.63 mg/g and 8.72, 20.86, 38.04 mg/g for 15, 50 and 120 mg/L of initial nitrate concentrations were obtained, respectively. As shown in Figs. 8 and 9, a relatively higher uptake value was observed for nitrate sorption on PHA-AE at higher initial concentrations of nitrate. A higher q_e was observed at higher concentrations in column test for nitrate removals that may be attributed to the concentration gradient. This will finally enhance the adsorption process. Similar results were reported in a work by Xing for the nitrate and phosphate removals by WS-AE and Han's work for methylene blue adsorption onto natural zeolite in a fixed-bed column [26,12]. The exhaustion time decreased with the increase of initial concentrations of nitrate. This behavior was due to the increase of the initial concentrations and the fact that the sites of adsorbent were filled quickly. Also, the exhaustion time decreased with increase of flow rate. Generally, for nitrate at higher flow rates, sharper breakthrough curves were obtained. The breakpoint time and total adsorbed nitrate quantity decreased with the increase flow rate. This behavior can be explained by the fact that nitrate sorption was affected by insufficient residence time of the solute in the column. The insufficient time decreases the bonding capacity of the nitrate ions onto aminated group

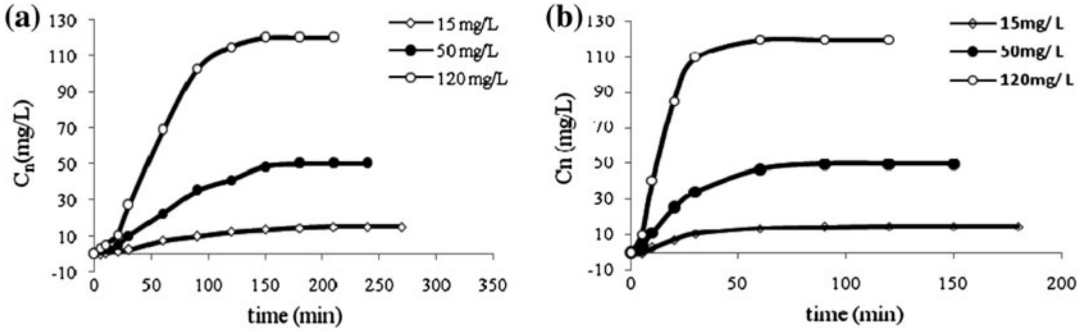

Fig. 8. The change of equilibrium nitrate concentration with time on PHA-AE micrometer-sized (flow rate: 0.98L/h and 2.27L/h, initial concentration of nitrate: 15, 50, and 120 mg/L, pH = 6).

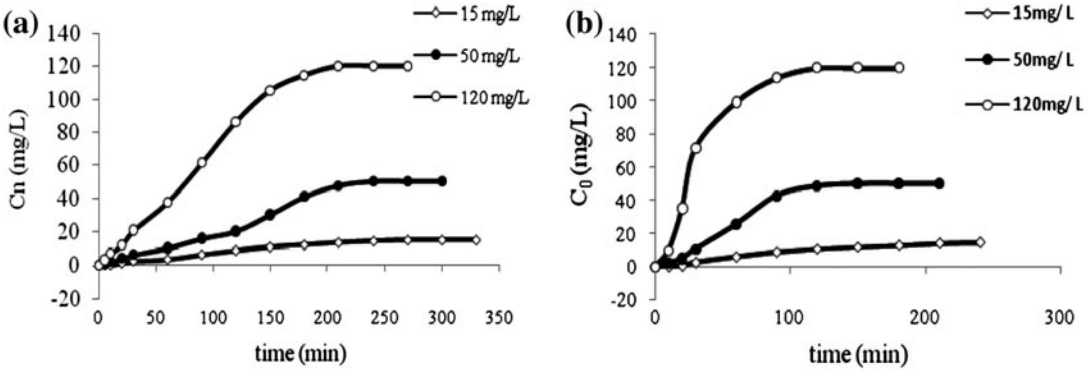

Fig. 9. The change of equilibrium nitrate concentration with time on PHA-AE nanometer-sized (flow rate: 0.98L/h and 2.27L/h, initial concentration of nitrate: 15, 50, and 120 mg/L, pH = 6).

present in the sorbent. It was suggested that lower flow rate would help nitrate sorption in the column tests.

5. Conclusion

The results of this study showed that the nitrate removal was optimal at pH 6. The equilibrium times were obtained as 180 and 120 min for micrometer and nanometer adsorbents, respectively. Higher initial nitrate concentrations led to lower removal percentages; however, higher adsorption capacities were obtained. As the adsorbent dose increased, the removal of nitrate increased, while the adsorption capacity decreased. Adsorption kinetics of nitrate ions onto PHA-AE may be most successfully described by the pseudo-second-order model. The adsorption behavior of nitrate ions followed Langmuir–Fruendlich isotherm. The breakpoint time and total adsorbed nitrate quantities also decreased with the increased flow rate of the solute in the column. The results allow us to conclude that PHA-AE represents promising adsorbent for the removal of nitrate anions from aqueous solutions even at high concentrations. Since PHA-AE-nanometer developed higher capacities of nanoparticles for removal of nitrate, it showed a higher capability of adsorbing nitrate as compared to PHA-AE-micrometer adsorbent.

Acknowledgments

The authors are thankful to Dr Labibzadeh, Department of Civil Engineering, Chamran University of Ahvaz, Assistant Professor and H. Hoseini, Department of Environmental health Engineering, modares University, Tehran, for their valuable helps.

References

[1] Y. Wang, B.Y. Gao, W.W. Yue, Q.Y. Yue, Adsorption kinetics of nitrate from aqueous solutions onto modified wheat residue, Colloids Surf. A 308 (2007) 1–5.

[2] K.T. Dhermendra, J. Behari, S. Prasenjit, Application of Nanoparticles in Waste Water Treatment, World Appl. Sci. J. 3 (2008) 417–433. ISSN 1818–4952.

[3] A.M.O. Mohamed, Development of a novel electro-dialysis based technique for lead removal from silty clay polluted soil, J. Hazard. Mater. 90 (2002) 297–310.

[4] N.J. Savage, Nanopart. Res. 7 (2005), 331–342. doi: 10.1007/s11051-005-7523-5.

[5] L. Thorneby, K. Persson, Treatment of liquid effluents from dairy cattle and pigs using reverse osmosis, J. Agric. Eng. Res. 74 (1999) 159–170.

[6] A. Uygur, F. Karg, Biological nutrient removal from pre-treated landfill leachate in a sequencing batch reactor, J. Environ. Manage. 71 (2004) 9–14.

[7] I. Fernandez-Olmo, J.L. Fernandez, A. Irabien, Purification of dilute hydrofluoric acid by commercial ion exchange resins, Sep. Purif. Technol. 56 (2007) 118–125.

[8] U.S. Orlando, T. Okuda, W. Nishijima, Chemical properties of anion Exchangers prepared from waste natural materials, React. Funct. Polym. 55 (2003) 311–318.

[9] R.M. Gong, Y. Ding, M. Li, Utilization of powdered peanut hull as biosorbent for removal of anionic dyes from aqueous solution, Dyes Pigm. 64 (2005) 187–192.

[10] P.K. Stoimenov, R.L. Klinger, G.L. Marchin, K.J. Klabunde, Metal oxide nanoparticles as bactericidal agents, Langmuir 18 (2002) 6679–6686.

[11] V.L. Colvin, The potential environmental impact of engineered nanomaterials, Nature Biotech. 10 (2003) 1166–1170.

[12] X. Xing, B. Gao, Q. Yue, Q.Q. Zhong, Preparation of agricultural by-product based anion exchanger and its utilization for nitrate and phosphate removal, Bioresour. Technol. 101 (2010) 8558–8564.

[13] J.A. Laszlo, Preparing an ion exchange resin from sugarcane bagasse to remove reactive dye from wastewater, Text. Chem. Col. 28 (1996) 13–17.

[14] J.J. Orfao, A.I. Silva, J.C. Pereira, S.A. Barata, I.M. Fonseca, P. C. Faria, M.F. Pereira, Adsorption of a reactive dye on chemically modified activated carbons–influence of pH, J. Colloid Interface Sci. 29 (2006) 480–489.

[15] R. Malekian, J. Abedi-Koupai, S.S. Eslamian, F. Mousavi, K. Abbaspour, M. Afyuni, Ion-exchange process for ammonium removal and release using natural Iranian zeolite, Appl. Clay Sci. 51 (2011) 323–329.

[16] U. Kumar, M. Bandyopadhyay, Sorption of cadmium from aqueous solution using pretreated rice husk, Bioresour. Technol. 97 (2006) 104–109.

[17] http://www.oakdaleengr.com/datafit.htm.

[18] K. Saltali, A. Sari, M. Aydin, Removal of ammonium ion from aqueous solution by natural Turkish (YIldIzeli) zeolite for environmental quality, J. Hazard. Mater. 141 (2007) 258–263.

[19] M. Shirvani, H. Shariatmadari, M. Kalbasi, Kinetics of cadmium desorption from fibrous silicate clay minerals: Influence of organic ligands and aging, Appl. Clay Sci. 37 (2007) 175–184.

[20] B.Y. Gao, X. Xu, Y. Wang, Q.Y. Yue, X.M. Xu, Preparation and characteristics of quaternary amino anion exchanger from wheat residue, J. Hazard. Mater. 165 (2009) 461–468.

[21] M. Ulmanu, I. Anger, Y. Fernandez, L. Castrillon, E. Maranon, Batch Chromium (VI), Cadmium (II) and Lead (II) Removal from Aqueous Solutions by Horticultural Peat, Water Air Soil Pollut. 194 (2008), 209–216. doi: 10.1007/s11270-008-9709-9.

[22] M. Sarioglu, Removal of ammonium from municipal wastewater using natural Turkish (Dogantepe) zeolite, Sep. Purif. Technol. 41 (2005) 1–11.

[23] L.C. Lei, X.J. Li, X.W. Zhang, Ammonium removal from aqueous solutions using microwave-treated natural Chinese zeolite, Sep. Purif. Technol. 58 (2008) 359–366.

[24] C. Raji, T.S. Anirudhan, Batch Cr (VI) removal by polyacrylamide-grafted Sawdust: kinetics and thermodynamics, Water Res. 32 (1998) 3772–3780.

[25] A. Rahmani, H. Zavvar Mousavi, M. Fazli, Effect of nanostructure alumina on adsorption of heavy metals, Desalination 253 (2010) 94–100.

[26] R.P. Han, Y. Wang, W.H. Zou, Y.F. Wang, J. Shi, Comparison of linear and nonlinear analysis in estimating the Thomas model parameters for methylene blue adsorption onto natural zeolite in fixed-bed column, J. Hazard. Mater. 145 (2007) 331–335.

[27] A. Ramesh, B.A. Devi, H. Hasegawa, T. Maki, K. Ueda, Nanometer-sized alumina coated with chromotropic acid as solid phase metal extractant from environmental samples and determination by inductively coupled plasma atomic emission spectrometry, Microchem. J. 86 (2007) 124–130.